Journal of Hydrology, 112 (1989) 1–18
Elsevier Science Publishers B.V., Amsterdam — Printed in The Netherlands

[2]

FIELD STUDIES OF THE EFFECTS OF THE CAPILLARY FRINGE ON STREAMFLOW GENERATION

A.S. ABDUL* and R.W. GILLHAM

Institute for Groundwater Research, University of Waterloo, Waterloo, Ont. N2L 3G1 (Canada)

(Received January 30, 1989; accepted after revision February 25, 1989)

ABSTRACT

Abdul, A.S. and Gillham, R.W., 1989. Field studies of the effects of the capillary fringe on streamflow generation. J. Hydrol., 112: 1–18.

Two field experiments were conducted to investigate the effect of the capillary fringe on surface water–groundwater interactions and on streamflow generation in a shallow water-table aquifer. The results from both experiments showed that the water-table adjacent to the stream, where the capillary fringe extended to or close to ground surface, responded rapidly to the precipitation events due to the initially low storage capacity of the medium. This rapid and large response led to the development of a water-table mound on both sides of the stream and flow nets showed that the mound resulted in the discharge of pre-event water through the seepage faces that developed on both sides of the stream. Furthermore, the mound contributed to the discharge of event water in that precipitation falling on the seepage faces was transported directly to the stream as overland flow. A further contribution of event water to the stream occurred as surface runoff from areas upslope of the seepage faces, where the pressure head was zero, but the rainfall rate exceeded the infiltration capacity of the soil. Under the conditions of the study, the results support the commonly recognized mechanisms of streamflow generation, including the partial area, variable-source-area overland flow, and variable-source-area subsurface flow concepts. The relative contribution of these mechanisms to stormflow appeared to be determined by the response of the capillary fringe. The amount of pre-event water in the discharge determined by the tracer method of hydrograph separation showed good agreement with the instantaneous pre-event discharge hydrograph determined from flow nets.

INTRODUCTION

During the past two decades, several studies have been conducted using chemical and isotopic tracers to separate stormflow hydrographs into event and pre-event components (Dincer et al., 1970; Martinec, 1975; Fritz et al., 1976; Sklash and Farvolden, 1979). In general, the results of these studies have shown that the contribution of pre-event water to streamflow is substantially greater than would be expected on the basis of most recognized mechanisms of streamflow generation. The results are of scientific interest in that they indicate an incomplete understanding of the mechanisms of streamflow

* Present address: Environmental Science Department, General Motors Research Laboratories, Warren, MI 48090 (U.S.A.)

generation and are of great practical importance with respect to the development of watershed models for predicting both quantity and quality of runoff. The results of the tracer studies have been slow to gain acceptance in the absence of any recognized mechanism to explain the large and rapid increase in pre-event water to a stream in response to a rainfall event. Several recent papers (Sklash and Farvolden, 1979; Gillham, 1984; Abdul and Gillham, 1984; Blowes and Gillham, 1988) have proposed that the capillary fringe could provide the necessary mechanism. The capillary fringe is the zone above the water-table that remains saturated under negative pressure. This zone has little or no storage capacity and when it extends to ground surface, the application of a small quantity of water can cause a rapid and large water-table rise. In near-stream areas, the water-table response could result in a rapid increase in subsurface discharge to the stream.

In detailed laboratory studies of the capillary fringe effect on streamflow generation, Abdul and Gillham (1984) showed that the zone of tension saturation could indeed result in a rapid rise in the water-table in response to precipitation events. The rise in the water-table resulted in increased hydraulic gradients towards the stream and an associated rapid increase in the discharge of pre-event water to the stream. It was further shown that the rising water-table generated a seepage face which tended to promote the overland flow of event water to the stream. The results showed that the proportions of pre-event and event water in the stream were dependent upon the intensity of the rainfall event, and based on the physical characteristics of the mechanism, it was further postulated that the proportions of event and pre-event water would be sensitive to surface slope and the texture of the geologic material. The results are of interest in that they provide a detailed physical description of the mechanism of streamflow generation, and also demonstrate that several mechanisms may contribute simultaneously. However, because of the small scale and artificial conditions under which the tests were conducted, the practical significance of the results remains uncertain.

The present study was undertaken to examine, under field conditions, the effect of the capillary fringe on the process of streamflow generation.

DESCRIPTION OF THE STUDY AREA

The study area selected for this investigation was located at Canadian Forces Base Borden, approximately 70 km NNW of Toronto, Ontario. The area in the vicinity of the test site is of low relief, is grass covered, and overlies a shallow sandy aquifer. MacFarlane et al. (1983) described the aquifer as being predominantly medium-grained sand of glaciofluvial origin. Small-scale bedding in the sand was noted, as well as occasional silty layers and lenses. From the results of several testing procedures, MacFarlane et al. (1983) reported the hydraulic conductivity of the aquifer to range from 1×10^{-2} to 3×10^{-3} cm s^{-1}.

A plan-view and two cross sections of the study site are given in Fig. 1. The

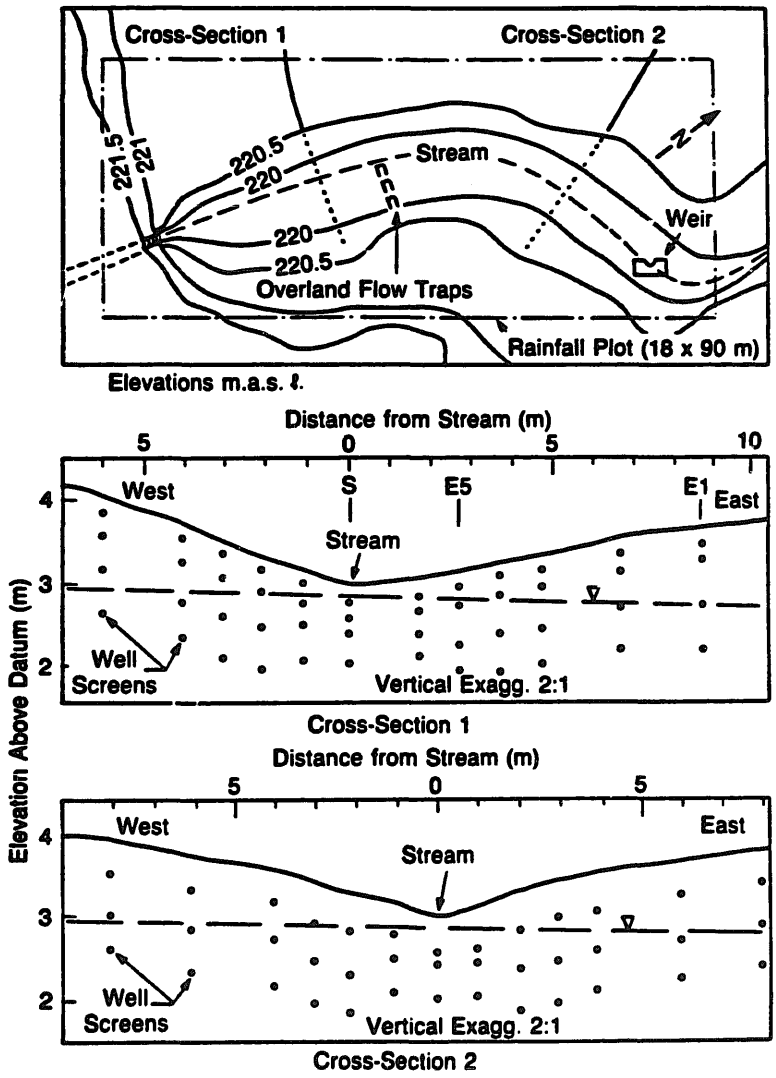

Fig. 1. Plan-view of the experimental site and schematics of cross-sections 1 and 2.

site is about 18 m wide by 90 m long, and is traversed by a man-made stream channel. Prior to the experiments, the grass cover was removed from the channel, giving a well-defined trapezoidal waterway that was about 60 cm wide with a mean slope of less than 1 degree. The stream channel is about 1.2 m below the elevation of the surrounding land and is formed by shallow banks having slopes that vary from about 4 to 9 degrees. Streamflow is intermittent, with the water-table varying annually from the stream surface to about 1 m below the stream bed.

Examination of soil samples collected during installation of piezometers showed the upper 10 to 20 cm to be an organic-rich sandy surface soil (A horizon), while at greater depth, the sand appeared to be very characteristic of the aquifer material described in MacFarlane et al. (1983). There was however, only minor evidence of small-scale bedding, and no silt layers or lenses were encountered.

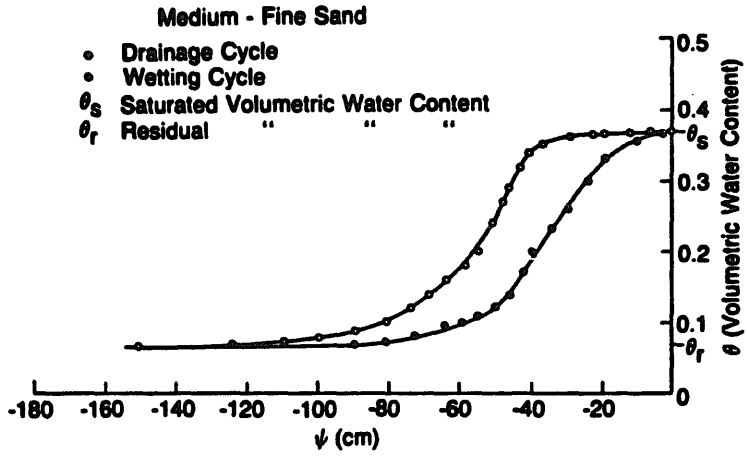

Fig. 2. Main drying and wetting curves for the aquifer material.

The volumetric water content–pressure head relationships for the sand as determined by a hanging water column method similar to that of Day et al. (1967), is shown in Fig. 2. The sand sample was placed in a fritted-disc buchner (Pyrex) funnel that was hydraulically connected to a fixed horizontal microburette. The main drainage and main wetting curves were determined by applying successive increments of negative pressure to an initially saturated sample and successive increments of less negative pressure to the fully drained sample, respectively. The water content corresponding to each value of negative pressure was calculated from the water content at the previous pressure head and the measured volume of water that drained from or entered the sand sample as a result of the incremental change in pressure. Referring to the main drainage curve of Fig. 2, the air entry value for the sand is about – 30 cm and the residual water content is reached at a pressure head of about – 120 cm. In a hydrogeologic context, this indicates that under static flow conditions, the soil would remain saturated for a distance of about 30 cm above the water-table, while the soil above 120 cm from the water-table would be at the residual water content (8%).

INSTRUMENTATION AND MONITORING

The experimental design involved measurement of the physical response of the groundwater zone and the chemical and physical response of surface runoff and streamflow to simulated rainfall containing a nonreactive tracer.

Changes in hydraulic head were monitored using 87 piezometers arranged in two cross-sections perpendicular to the stream (Fig. 1). Each piezometer was made from 4 cm I.D. PVC pipe that was capped at the base and slotted over 10 cm from a point 5 cm above the base. The slotted region was wrapped with 210 μm Nytex screen. Changes in the position of the water surface in each well was determined from the displacement of a calibrated rod that was attached to a ping-pong ball which floated on the water in each well (Fig. 3). The initial

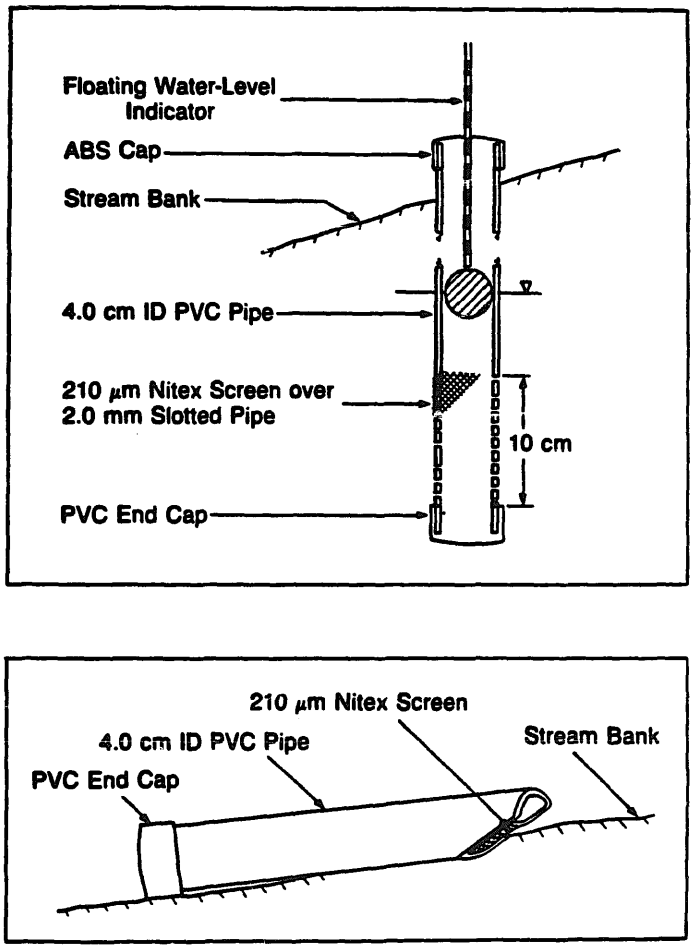

Fig. 3. Schematics of the piezometer and overland flow catcher.

elevation of the water level was determined using a water level tape. In cross-section 1, the up-stream cross-section, there were twelve nests. each having four piezometers. In general, the centers of the slotted region of the piezometers at each nest were 15, 40, 90, and 140 cm below ground surface and the first three nests on either size of the stream were 1 m apart while the others were 2 m apart. Cross-section 2, the downstream cross-section, had thirteen nests of three piezometres. The layout of these piezometers was similar to that of section 1 except that the shallowest piezometer (15 cm) was not installed. All the piezometers were developed several times during the period of a month by pumping out the standing water. The change in water level in each piezometer was read at about 10-min intervals during the experiment.

A 90-degree V-notch weir was installed at the downstream end of the study area. To prevent water from ponding and backing up in the stream, the spout of the weir was at the same level as the stream bed. Stream discharge was measured and sampled at 5-min intervals during the discharge period.

During the precipitation event, samples of surface flow at several locations on the east slope of section 1 and of streamflow at section 1 were collected at

10-min intervals. A schematic of the surface collectors is shown in Fig. 3, and the positions of the collectors on the east slope are shown in Fig. 1. Each surface collector was made of 4 cm I.D. PVC pipe that was capped at the lower end. The other end of the pipe has a 45° sloped opening to shield off direct precipitation and the lower half of this opening was wrapped with 210 μm Nytex screen to filter debris from the sample. The collectors, positioned a few millimetres below ground surface, were emptied after sampling.

Rainfall was simulated by a sprinkler irrigation system that was connected to a nearby fire hydrant. The irrigation system consisted of eight lengths of aluminum pipe, 9 m long with a 7.5 cm I.D., and nine Nelson sprinkers. The sprinklers were attached to the ends of the pipes and an individual sprinkler irrigated a circular area of 9 m radius. The instrument area was 14 m wide and 70 m long and was therefore contained within the irrigated plot. Rainfall rate was controlled by a booster pump connected in series with the hydrant and irrigation system, and a nonreactive tracer (bromide) was injected into the "event water" by means of a high-pressure pump located between the booster pump and the first sprinkler. Average rainfall rates were determined from several rainfall collectors distributed over the study area. The concentration of bromide in the rainfall was determined from samples taken from the rainfall collectors at the end of the storm and from samples collected at 10-minute intervals from a larger collector in the center of the test plot. Both the total rainfall and the concentration of bromide in the rainwater were quite uniform over the study site.

Two experiments were conducted at the site. For the first of these (event 1), the initial readings from the piezometers showed no vertical hydraulic gradients, and the water-table to be almost flat, but with a uniform slope of about 0.5 degrees toward the east. Initially there was no flow in the channel, and the depth to the water-table beneath the channel at cross section 1 was 22 cm. Referring to the water content–pressure head relation of Fig. 2, and the cross sections of Fig. 1, it appears that the capillary fringe would extend to ground surface for a distance of 1 m or more on either side of the stream, with the degree of desaturation increasing with greater distance from the stream. Where the ground became level, at distances of about 7 to 10 m from the stream, the depth to the water-table was greater than 1.0 m and thus, from Fig. 2, the surface soil in these regions would be approaching the residual water content. It should be noted that these experiments were conducted in late fall, a period of low evapotranspiration, and there had not been significant precipitation for a period of at least one week prior to the experiment.

Water samples collected from the piezometers prior to the rainfall showed no detectable bromide. The simulated rainfall was applied at a rate of 2.0 cm h^{-1} for a period of 50 min, and contained bromide at a concentration of 90 mg l^{-1}. Monitoring commenced with the initiation of rainfall, and continued for about 2 h after the rainfall ceased.

Experiment 2 (event 2) was similar to experiment 1; however, the initial water-table at cross section 1 was about 36 cm below the stream channel. In this

case a zone of partial saturation exist along the entire cross section, though in the near-stream area, the storage capacity of the unsaturated zone would be small. Rainfall was applied at a rate of 2.5 cm h^{-1} for a duration of 1.3 h and contained bromide at a concentration of 100 mg l^{-1}.

RESULTS AND DISCUSSIONS

In general, the two experiments give similar results. Experiment 1 will be considered in detail and when differences between the results of the two events were noted, the specific results of experiment 2 will be considered.

Hydraulic head response

In this section, the hydraulic-head response to the two precipitation events of six piezometers on the east slope of cross section 1, is considered. It should be noted that the response of the other piezometers in cross sections 1 and 2 was consistent with the results presented below.

The hydraulic head response of the six piezometers to event 1 is shown in Fig. 4. Piezometers S-2 and S-3 were located below the stream bed at depths of 38.1 and 51.0 cm respectively; piezometers E5-1 and E5-2 were 2.7 m from the center of the stream and at depths of 16.6 and 41.5 cm below ground surface, respectively; while piezometers E1-3 and E1-4 were 8.7 m from the center of the stream and at depths of 91.5 and 139 cm, respectively. Zero time is the time at which rainfall started and hydraulic head values are relative to an arbitrary zero datum 3 m below the stream bed. The initial hydraulic head values for

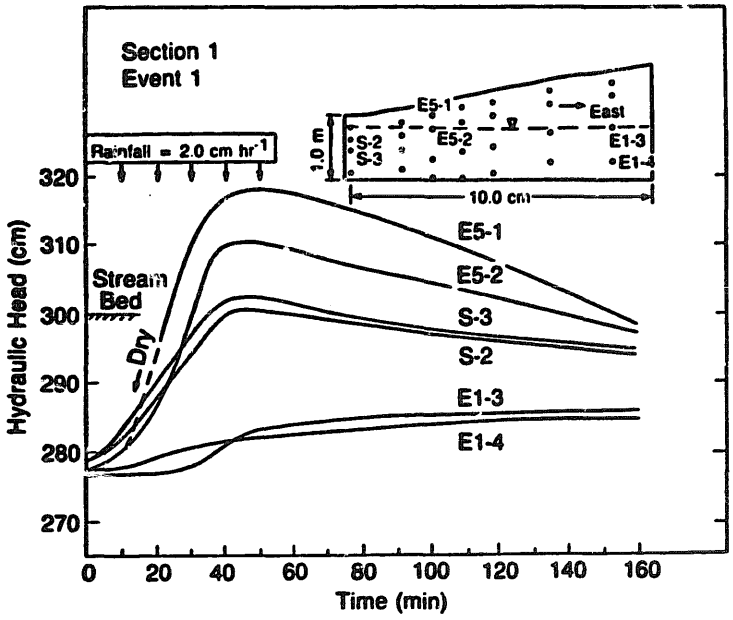

Fig. 4. Hydraulic head response of six piezometers located in the stream and on the east slope of section 1 for event 1.

piezometers of a particular nest were identical, indicating the initial absence of vertical hydraulic gradients, while the different head values at the different nests reflect the easterly flow of groundwater referred to previously.

Piezometers S-2 and S-3 responded in a similar manner, and immediately to the rainfall. The hydraulic head values increased by more than 20 cm in 40 min, then decreased at a much slower rate after the rain stopped. At a time of about 40 min, the hydraulic head values for both piezometers were greater than the elevation of the stream bed. The magnitude of the hydraulic head at S-3, the deeper piezometer, was always greater than at S-2, and at the time of maximum response there was an upward hydraulic gradient of 0.2, indicating the discharge of groundwater to the stream.

The response of piezometers E5-1 and E5-2 lagged the start of the rainfall event by about 5 min. Prior to the rainfall event the water table of nest E5 was 58 cm below the ground surface and based on the moisture content–pressure head relationship of Fig. 2, the surface soil was unsaturated with a volumetric water content of approximately 0.27. The delay in response was therefore attributed to the initial storage capacity of the unsaturated soil and the time required for water to percolate to the top of the capillary fringe. The response at nest E5, once started, was more rapid than at nest S, and the hydraulic head at E5 exceeded that at S after a time of about 20 min. With the cessation of rainfall, the hydraulic-head values at E5 declined slowly, almost paralleling the decline at nest S. The maximum response was 40 and 33 cm for E5-1 and E5-2, respectively.

The hydraulic gradients at nest E5 were downward throughout the experiment, reaching a value of 0.3 at the time of maximum response (about 50 min). This indicates that E5 was under recharge conditions throughout the experiment, compared with the discharge conditions noted previously at S. Also, based on Fig. 4, after the first 20 min of the rainfall event, there was a horizontal component of flow from E5 towards S.

The hydraulic head response of piezometers E1-3 and E1-4 are significantly lagged and subdued relative to the response at nests S and E5. Initially, the water table was 92 cm below the ground surface at E1 and therefore, from Fig. 2, the surface soil was unsaturated with a volumetric water content of approximately 0.08. The infiltrating water during the rainfall event was therefore stored as a wetting front in the unsaturated zone. The upward gradients at E1 at early time may reflect the effects of the greatly increased hydraulic head values near the toe of the slope, while the downward gradients at a later time (after about 40 min) may reflect the appearance of the wetting front at the saturated zone. The maximum hydraulic head response at E1 was about 7 cm.

In event 2, the water-table below the stream at section 1 was initially at a depth of about 35 cm. Although the water-table position was deeper than that of event 1, Fig. 2 shows that the capillary fringe initially extended close to the bed of the stream. In this event, the rainfall rate of 2.5 cm h^{-1} is approximately 1.3 times greater than the rainfall rate of event 1.

The hydraulic head response of nests S, E5, and E1 for event 2 are shown in

Fig. 5. These results are similar to those of event 1 (Fig. 4) in that nests S and E5 show an early and large response to the rainfall event, while nest E1 shows a delayed and much lower response. However, due to the greater initial depth to the water-table and the higher rate of water application, the magnitude of the responses at S and E5 are greater than those for event 1. As in experiment 1, location S was under discharge conditions, at least until a time of about 120 min, and E5 was under recharge conditions throughout the experiment. Also, there was a horizontal component of flow from E5-1 in the direction of S.

Water-table response

Because of the highly transient nature of the response and the 10 min frequency of the water-level readings, in order to determine the position of the water-table at a particular time, the hydraulic head values were first plotted as a function of time for all piezometers, and the hydraulic-head values at selected times were read from the graph. The pressure head profile was then determined at each piezometer nest and at each of the selected times by subtracting the elevation head of the respective piezometers from the corresponding hydraulic head values. The extrapolation of the profile to zero pressure head gave the position of the water-table at each piezometer nest and at each of the selected values of time. The interpolation of the hydraulic-head data and the extrapolation of the pressure head data were over relatively short intervals of time and space, respectively; nevertheless, these procedures would lead to some degree of uncertainty in the calculated positions of the water-table. Though additional

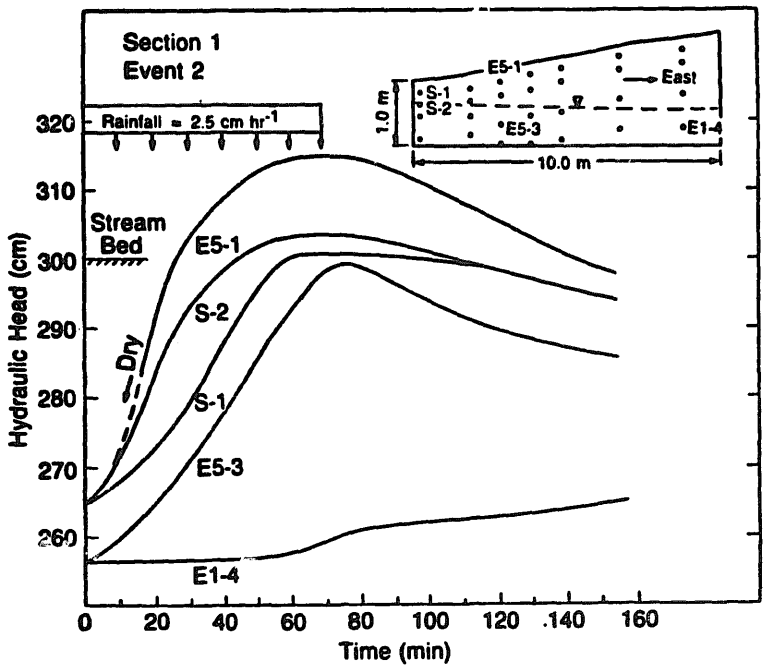

Fig. 5. Hydraulic head response of five piezometers located in the stream and on the east slope of section 1 for event 2.

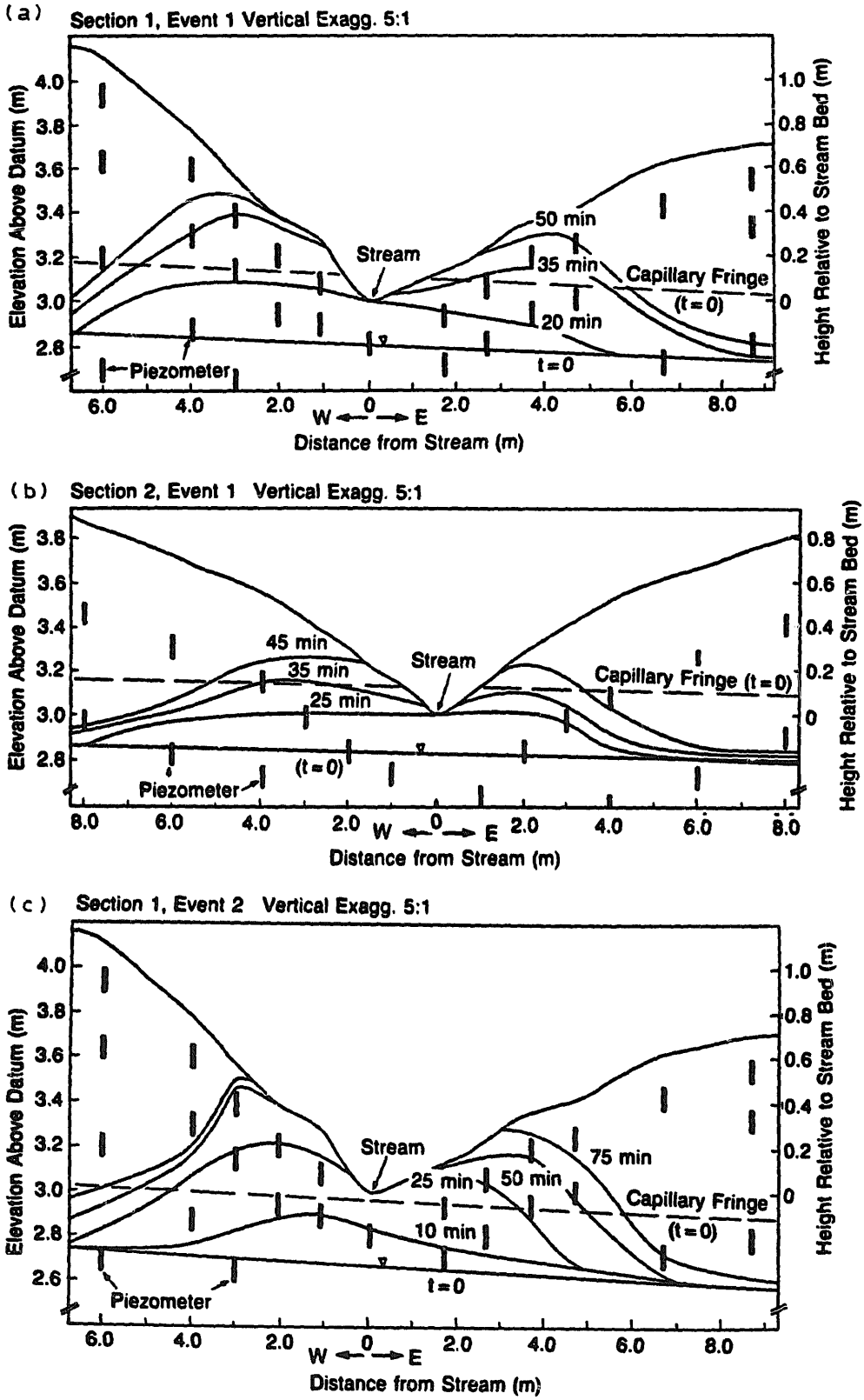

Fig. 6. (a) Water-table response, section 1–event 1; (b) water-table response, section 2–event 1; (c) water-table response, section 1–event 2.

uncertainty can be attributed to a lag in the response of the piezometers, from the consistency of the data, it was felt that the position of the water-table could be determined quite reliably within ± 2 cm.

The water-table positions at different times for cross-sections 1 and 2 of event 1, and for cross-section 1 of event 2 are shown in Fig. 6. For both events and both cross-sections the initial water-table was relatively flat and sloping from west to east. As observed for the hydraulic-head data, the magnitude and rate of the water-table response is strongly dependent upon the position in the flow system.

Figure 6a shows the water-table positions at four different times for cross-section 1–event 1. About 20 min after the rain started, the water-table below and adjacent to the stream had risen about 20 cm to the elevation of the stream bed, and 15 min later, a water-table mound extended upslope on both sides of the stream. Away from the stream, where the surface soil was initially unsaturated and at low moisture content, the response of the water-table was quite small. The water-table response for section 2 of event 1 (Fig. 6b) is consistent with that at section 1.

The water-table response for section 1–event 2 is shown in Fig. 6c. Because of the greater initial depth to the water-table, the magnitude of the response near the stream is much greater than observed for event 1. Although the storage capacity of the medium was greater than in event 1, the extent of the water-table mound was similar to that of event 1 due to the higher application rate and longer duration of event 2. The sharper decline at the shoulders of the water-table mound can probably be attributed to the initially dryer conditions in the region near the stream in event 2.

The temporal and spatial variations in the hydraulic-head and water-table responses can only be explained by invoking the principles of the capillary fringe. If a specific yield value typical of a medium sand (about 0.25) is used, then assuming no downward flow in the saturated zone, which was clearly not the case, then the application of 1.7 cm of water would give a maximum rise in the water-table of 6.8 cm. This is substantially less than the maximum rise of about 60 cm in Fig. 6a. The rapid and disproportionate rise can only be attributed to a reduced storage capacity in the zone above the water-table. Based on Fig. 2, it is clear that this reduced storage is the result of water being retained by capillary forces, resulting in volumetric water content values that are substantially above the residual value. Where the zone of tension saturation (the capillary fringe) extends to ground surface, there is virtually no storage capacity and thus the application of a relatively small amount of water results in a large rise in the water table.

With respect to the objectives of this study, the shape of the resulting water-table mound is of particular importance. With the initial water-table close to the stream bottom (Fig. 6a for example) the maximum rise in the water-table is limited by the elevation of the stream. With increasing surface elevation away from the stream, the water-table response is greater, but is still limited by the surface elevation. At greater distances from the stream, the

surface elevation exceeds the elevation of the top of the capillary fringe, and thus the storage capacity of the soil increases with greater distance. This is reflected in Fig. 6 by the rapid decrease in the maximum water-table elevation at distances greater than about 4 m from the stream.

It is clear that the generation of the water-table mound adjacent to the stream can influence streamflow generation in two ways. The peak of the mound will act as a groundwater divide, causing groundwater to flow toward the stream and also in directions away from the stream. This is shown in the water-table positions of Fig. 6 and also in the hydraulic-head data of Figs. 4 and 5. Secondly, the rising water-table will cause surface saturation in the near-stream areas, which will tend to promote surface runoff. The interactions of these mechanisms will be examined in the following sections.

Stream-flow response

The bromide added to the rainwater of events 1 and 2, was used to separate the storm hydrograph into event and pre-event components. In the case of event 2, because of the initially low water-table position below the stream, there was significant storage of event-water in the porous medium away from the stream prior to the start of stream discharge. A separation of the storm hydrograph by the tracer technique would therefore be inaccurate for the initial conditions of event 2; therefore, the results of the hydrograph separation by this technique will not be presented.

Using the mass balance method, and because the background bromide concentration was less than 1 mg l^{-1}, the event component in the stream discharge is simply the product of the stream discharge and the ratio of the bromide concentration in the stream discharge to the rainfall concentration (90 mg l^{-1}).

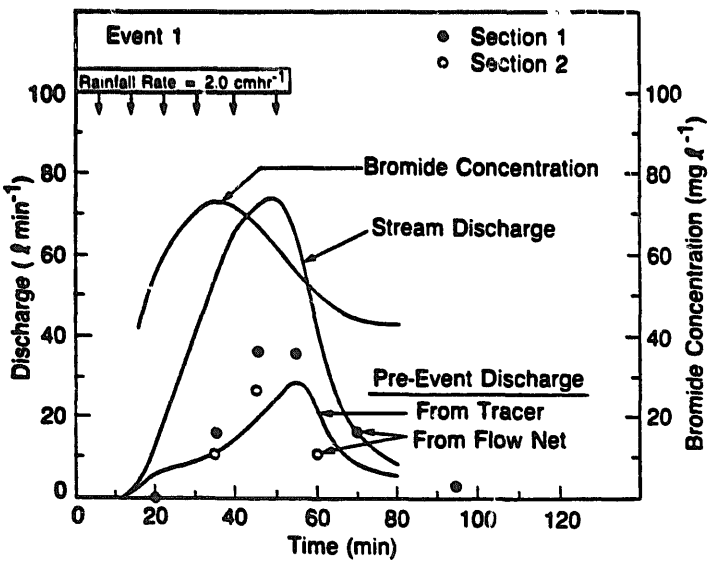

Fig. 7. Stream and pre-event discharge hydrographs and concentration of bromide in the stream discharge for event 1.

Figure 7 shows graphs of stream discharge and bromide concentration in the stream discharge versus time for event 1 as measured at the downstream weir. Discharge at the weir started about 15 min after the initiation of rainfall, although surface saturation and some ponding was observed at many locations along the length of the stream about 5–10 min after the start of the rainfall event. The stream discharge increased rapidly and steadily to a peak value of 74 l min^{-1} at the time the rainfall event stopped and then decreased at a similar rate over the next 20 min. After this time, the stream discharge decreased more gradually.

The graph of bromide concentration in the stream discharge versus time has a shape similar to that of the discharge hydrograph, with the initial concentration of 42 mg l^{-1} (47% of rainfall concentration) and a maximum of 72 mg l^{-1} (80% of rainfall concentration). The peak bromide concentration occurred 15 min before the peak discharge indicating that at this time the relative proportion of pre-event to event water was increasing with time.

The pre-event hydrograph is included in Fig. 7. This figure shows that the discharge of pre-event water commenced at the same time as the stream discharge and during the first 10 min of discharge, pre-event water made up approximately 50% of the streamflow. Later, stream discharge increased much faster than the discharge of pre-event water and at about 25 min after streamflow was first observed, pre-event water made up about 18% (15 l min^{-1}) of the stream discharge. After this time, the discharge of pre-event water increased at about the same rate as the stream discharge and reached a peak value of 28 l min^{-1} or 38% of the total discharge at the time of peak discharge. The shape of the pre-event discharge hydrograph is probably due to the variation in surface slope (4°–9°) adjacent to the stream. The regions of low slopes will respond sooner and come to equilibrium at an earlier time than the regions of larger slopes. However, because of the larger groundwater gradients associated with steeper slopes, they have the potential to discharge larger quantities of pre-event water than regions of low slopes.

Figure 8 shows graphs of bromide concentration versus time for streamflow at section 1 and for overland flow at two locations on the east slope of section 1. The shape and magnitude of the bromide concentration versus time for the stream discharge at section 1 are similar to those of the stream discharge at the downstream weir.

The overland flow at the point 2.7 m from the center of the stream, on the east slope of section 1, contained 100% event water for all times at which samples could be collected, while at the point 1.5 m from the stream, the pre-event component of the surface runoff increased from 10 to 18%. These results indicate that surface runoff was occurring for a distance in excess of 2.7 m from the stream, and consistent with the water-table position of Fig. 6a, indicate that the surface was saturated and at zero pressure head over this distance. The fact that all the water was event water indicates that there was no groundwater discharge at a distance of 2.7 m from the stream and that the overland flow was the excess of precipitation over infiltration. The occurrence of pre-event water

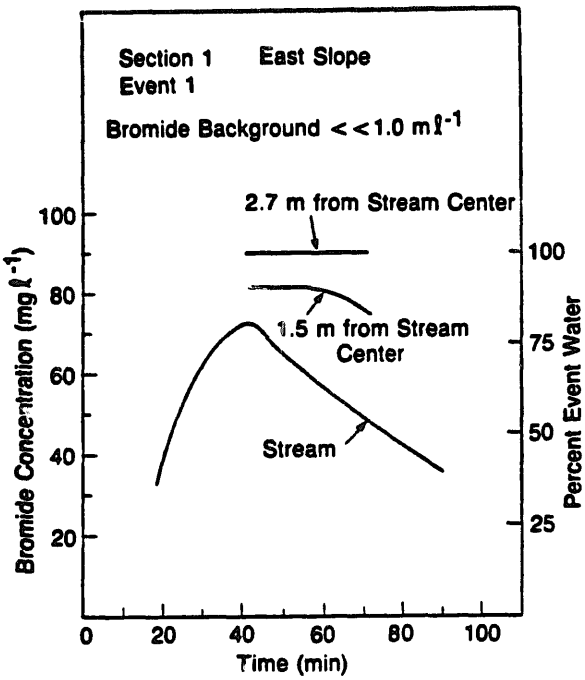

Fig. 8. Bromide concentration in the streamflow at section 1 and in the overland flow at two points on the east slope of section 1 for event 1.

in the surface runoff collected at a distance of 1.5 m from the stream indicates that the seepage face (zero pressure head with outwardly directed hydraulic gradients) extends for a distance beyond 1.5 m from the stream. These results are consistent with the laboratory results reported in Abdul and Gillham (1984) and will be confirmed by the flow-net analyses in the following section.

The stream discharge hydrograph of event 2 (Fig. 9) differs from that of event 1 in several ways. Because of the greater initial depth to the water-table, the start of stream discharge lagged the start of the rain by about 30 min, compared with less than 15 min for event 1. Further, the larger rainfall rate of event 2 (2.5 cm h^{-1}) resulted in a steeper increase in discharge and a higher discharge peak (97 l min^{-1}) than observed for event 1 (74 l min^{-1}).

Flow-net analysis

The hydraulic head values from the 87 piezometers of sections 1 and 2 were used to construct several flow nets for a number of times during events 1 and 2. The flow nets for both cross-sections and for events 1 and 2 show similar trends and therefore only four of these flow nets are shown in Fig. 10, three for section 1–event 1 and one for section 1–event 2.

The flow nets of section 1–event 1 show that the hydraulic gradient towards the stream increased with time and reached a maximum at the time the rain stopped. Because of its steeper surface slope and faster rate of response the west side of section 1 developed larger hydraulic gradients that the east slope,

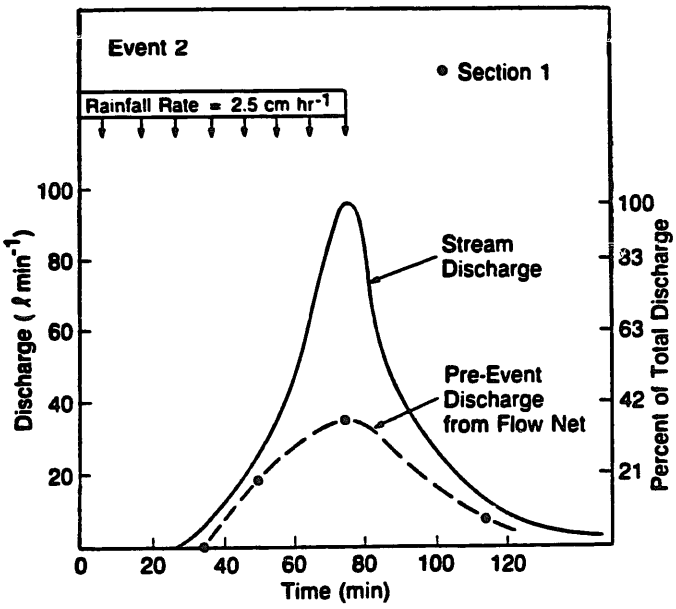

Fig. 9. Stream and pre-event discharge hydrographs for event 2.

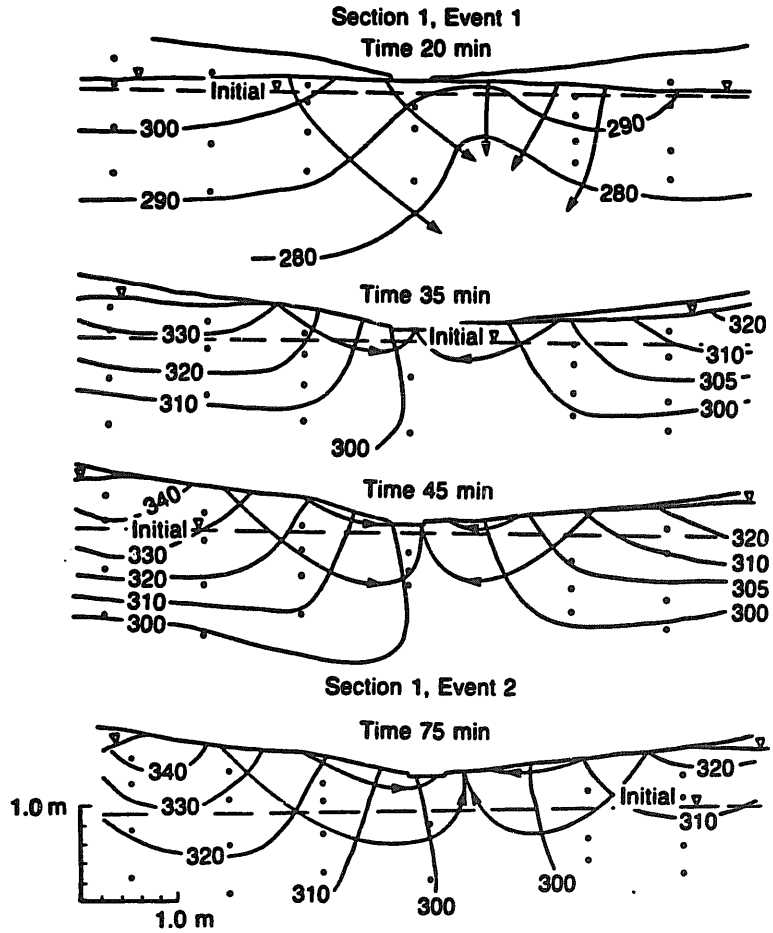

Fig. 10. Flow nets at section 1 for events 1 and 2.

resulting in an easterly displacement of the hydraulic divide beneath the stream. Consequently, the subsurface discharge from the west side was consistently larger than from the east side.

Because of the complex flow geometry and the limited amount of data, construction of quantitative flow nets that were consistent throughout the flow domain was extremely difficult. Aiming at what appeared to be reasonable distributions of the equipotential lines and flow lines, the total subsurface discharge to the stream was obtained from the sum of discharges calculated for the individual stream tubes.

As stated previously the measured values of hydraulic conductivity for the aquifer vary by almost an order of magnitude, from 3×10^{-3} to 1×10^{-2} cm s^{-1}. This range of values could of course, result in calculated subsurface discharge values that vary over a similar range. A value of 5×10^{-3} cm s^{-1} was used in the following calculation because it was the most commonly measured value and is reasonably close to the mean. The subsurface discharge from an individual cross-section was multiplied by the length of the reach (70 m) to determine the approximate total subsurface discharge at the weir. These results are shown in Fig. 7 for event 1 and in Fig. 9 for event 2.

The steeper slope and the faster response of the west side of section 1 led to consistently greater discharge through this section than through section 2. The subsurface discharge calculated from the flow nets of both cross-sections 1 and 2 for event 1 show trends that are similar to the trend calculated using the bromide tracer. However, discharge determined from the flow nets started about 10 min later and in general is greater than determined using the tracer. Considering the uncertainty in the hydraulic conductivity, as well as in the precise form of the flow nets, the agreement between the flow-net and tracer values of subsurface discharge is remarkably good, and indeed, may be fortuitous to a degree. Nevertheless, the similarity both in form and in magnitude, provides a considerable degree of confidence in the interpretation of the physical data.

Included in Fig. 10 is the flow net at the time of peak discharge for section 1–event 2. This flow net is similar to that of section 1–event 1 at the time of peak discharge. Although the peak subsurface discharge of event 2 (36 l min^{-1}) is greater than that of event 1 (28 l min^{-1}) its percent of the peak stream discharge is about the same (37%) as that of event 1 (38%).

SUMMARY AND CONCLUSIONS

The results of this study show that the water table adjacent to the stream responded immediately and rapidly to the rainfall of both events 1 and 2. In event 1, with an initially shallow water table, the capillary fringe extended from the water table to ground surface for some distance on both sides of the stream. Therefore the rapid water-table response was a result of the initially small storage capacity in the porous medium. Further away from the stream where the surface soil was initially unsaturated and at low moisture content,

the rate and magnitude of the water-table response was much lower. A similar response in event 2, when the entire surface was initially unsaturated, was due to the near-saturated surface conditions and associated small storage capacity adjacent to the stream.

The rapid and large response of the water table to the rainfall events led to the development of a water-table mound on both sides of the stream. Based on the flow nets, it is apparent that the water-table mound resulted in the discharge of pre-event water through the seepage faces that developed on both sides of the stream. Furthermore, the mound contributed to the discharge of event water in that precipitation falling on the seepage face was transported directly to the stream as overland flow. A further contribution of event water to the stream occurred as surface runoff from areas upslope of the seepage faces, where the pressure head was zero, but the rainfall rate exceeded the infiltration capacity of the soil. The flow nets clearly showed the effect of the rapid water-table rise in generating the subsurface discharge to the stream. A comparison of the water-table response of cross-sections 1 and 2 showed that the potential for pre-event discharge increases as the surface slope is increased. When the water-table extends to the surface, the steeper slopes resulted in larger lateral hydraulic gradients and therefore greater subsurface discharge to the stream.

The pre-event component discharge hydrograph at the weir, as determined by the tracer method of hydrograph separation, showed good agreement with the pre-event discharge hydrograph determined from the successive flow nets. Though there is a significant degree of uncertainty in the discharge calculated from the flow nets, the similarity in form and magnitude of the discharge determined from the flow nets and the tracer separation of the discharge hydrograph suggests that the water-table response could indeed account for the significant proportion of pre-event water (about 37%) in the stream discharge.

The results of this investigation are entirely consistent with the results obtained from the laboratory model (Abdul and Gillham, 1984), demonstrating, that at the field scale, the capillary fringe can indeed play an important role in the generation of streamflow. In particular, under the conditions of the study, the results support the previously proposed mechanism of streamflow generation including the partial-area, variable-source-area overland flow, and variable-source-area subsurface flow concepts. The response of the capillary fringe is, however, shown to be the mechanism responsible for these processes. The rise in the water-table generates the hydraulic gradients necessary for the rapid increase in the discharge of pre-event water to the stream (variable-source-area subsurface flow), and at the same time, results in the free-water condition at the surface that is necessary to generate overland flow (partial-area and variable-source-area concepts). The results suggest that no single mechanism is responsible for the generation of streamflow, and that under a given set of conditions, several mechanisms may interact simultaneously. Under shallow water-table conditions, the capillary fringe provides the

physical explanation for parts of the runoff mechanisms and is important in evaluating the relative importance of the various mechanisms under a given set of hydrogeologic and hydrologic conditions. Further work is required to evaluate the generality of these results.

ACKNOWLEDGMENTS

We wish to thank the many graduate students who helped with the monitoring during the experiments, and we appreciate the cooperation and help provided by the Department of Civil Engineering, Canadian Force Base Borden. In particular we wish to thank John Cherry for his helpful comments, Rob Higginson and Ray Carter for their assistance with the field work and data preparation, Marilyn Bisgould for typing this manuscript and Nadia Bahar for the drafting. Financial support for this study was provided by the Environmental Research Branch of the Chalk River Nuclear Laboratories of Atomic Energy Canada, Ltd.

REFERENCES

Abdul, A.S. and Gillham, R.W., 1984. Laboratory studies of the effects of the capillary fringe on streamflow generation. Water Resour. Res., 10(6): 691–698.

Blowes, B.W. and Gillham, R.W., 1988. The generation and quality of streamflow on uranium tailings near Elliot Lake, Ontario. J. Hydrol., 17: 1–23.

Day, P.R., Bolt, G.H. and Anderson, D.M., 1967. Nature of soil water. In: R.M. Hagan, H.R. Haise and T.W. Edminster (Editors), Agronomy, 9: 193–208, Am. Soc. Agron., Madison, Wisc.

Dincer, T., Payne, B.R., Florkowski, T., Martinec, J. and Tongiorgi, E., 1970. Snow-melt runoff from measurements of tritium and oxygen-18. Water Resour. Res., 6(1): 110–124.

Fritz, P., Cherry, J.A., Weyer, K.V. and Sklash, M.G., 1976. Runoff analyses using environmental isotopes and major ions. In: Interpretation of Environmental Isotopes and Hydrochemical Data in Groundwater Hydrology. International Atomic Energy Agency, Vienna, pp. 111–130.

Gillham, R.W., 1984. The effect of the capillary fringe on water-table response. J. Hydrol., 67: 307–324.

Martinec, J., 1975. Subsurface flow from snow-melt traced by tritium. Water Resour. Res., 11(3): 496–498.

MacFarlane, D.S., Cherry, J.A., Gillham, R.W. and Sudicky, E.A., 1983. Migration of contaminants in groundwater at a landfill: A case study 1. Groundwater flow and plume delineation. In: J.A. Cherry (Guest Editor), Migration of Contaminants in Groundwater at a Landfill: A Case Study. J. Hydrol., 63: 1–29.

Sklash, M.G. and Farvolden, R.N., 1979. The role of groundwater in storm runoff. J. Hydrol., 43: 45–65.